# Coulomb expansion of a thin dust cloud observed experimentally under afterglow plasma conditions © ©

Cite as: Phys. Plasmas **29**, 113705 (2022); https://doi.org/10.1063/5.0112680 Submitted: 21 July 2022 • Accepted: 11 October 2022 • Published Online: 10 November 2022

D Neeraj Chaubey and D J. Goree

# COLLECTIONS

- F This paper was selected as Featured
- This paper was selected as Scilight









#### ARTICLES YOU MAY BE INTERESTED IN

Keeping fine particles aloft in a plasma afterglow Scilight 2022, 461113 (2022); https://doi.org/10.1063/10.0015233

Barkas effect in strongly magnetized plasmas

Physics of Plasmas 29, 112103 (2022); https://doi.org/10.1063/5.0121285

The guiding effect of artificially injected gas bubble on the underwater pulsed spark discharge and its electrical and acoustic parameters after breakdown

Physics of Plasmas 29, 113504 (2022); https://doi.org/10.1063/5.0122080





# Coulomb expansion of a thin dust cloud observed experimentally under afterglow plasma conditions (1) (3)

Cite as: Phys. Plasmas 29, 113705 (2022); doi: 10.1063/5.0112680 Submitted: 21 July 2022 · Accepted: 11 October 2022 · Published Online: 10 November 2022







Neeraj Chaubey<sup>a)</sup> (D) and J. Goree (D)





## **AFFILIATIONS**

Department of Physics and Astronomy, University of Iowa, Iowa City, Iowa 52242, USA

<sup>a)</sup>Author to whom correspondence should be addressed: neeraj-chaubey@uiowa.edu

#### **ABSTRACT**

The Coulomb expansion of a thin cloud of charged dust particles was observed experimentally, in a plasma afterglow. This expansion occurs due to mutual repulsion among positively charged dust particles, after electrons and ions have escaped the chamber volume. In the experiment, a two-dimensional cloud of dust particles was initially levitated in a glow-discharge plasma. The power was then switched off to produce afterglow conditions. The subsequent fall of the dust cloud was slowed by reversing the electric force, to an upward direction, allowing an extended observation. At early time, measurements of the Coulomb expansion in the horizontal direction are found to be accurately modeled by the equation of state for a uniformly charged thin disk. Finally, bouncing from the lower electrode was found to be avoided by lowering the impact velocity <100 mm/s.

© 2022 Author(s). All article content, except where otherwise noted, is licensed under a Creative Commons Attribution (CC BY) license (http:// creativecommons.org/licenses/by/4.0/). https://doi.org/10.1063/5.0112680

# I. INTRODUCTION

A dusty plasma, also known as a complex plasma, consists of small solid particles along with electrons, ions, and neutral gas. <sup>1-9</sup> In the laboratory, a dusty plasma is commonly prepared starting with a glow-discharge plasma, sustained, for example, by direct current or radio frequency power, and introducing some powder by dropping it from above. 1-9,17-19 The dust particles gain a negative charge and can be levitated in an electric sheath above a lower electrode that has a negative potential. Prepared this way, the dust cloud can fill either a threedimensional volume 10-16,20 or a single two-dimensional horizontal plane,<sup>21–36</sup> depending on the experimental design.

When the power that sustains a glow discharge is switched off, there will be a temporal afterglow plasma, which has a lifetime of order 10<sup>-3</sup> s before electrons, and then ions escape to the chamber walls. 13-15,37-56 We can identify three times of great interest in a temporal afterglow: a transition to a condition where ions greatly outnumber electrons (this is commonly modeled as the end of ambipolar transport),<sup>38–41</sup> a transition where the charge on a dust particle frozen, which has also been quantified in models, <sup>38–41</sup> and, finally, the impact of the dust particle after it falls. The first two transitions generally occur within a few milliseconds, or even hundreds of microseconds, after the power that sustains the plasma is turned off. The impact of the dust particle can occur much later, depending on its starting height and acceleration. The dust particle's charge, which was generally negative during the steady operation of the plasma, can change polarity and become positive after the first transition mentioned above, due to a greater relative abundance of ions, compared to electrons.<sup>52</sup>

In addition to this kind of temporal afterglow, which is a transient condition due to turning off the power that sustains the plasma, there are also reports of spatial afterglows. These conditions, which can be sustained rather than transient, are found in the exhaust of flowing plasma. In these spatial afterglows, the conditions can be nonneutral, with a partial deficit of electrons, so that dust particles can charge positively there.<sup>5</sup>

For afterglow conditions, one topic of interest is the Coulomb expansion of the dust cloud. This expansion is sometimes termed a Coulomb explosion. 10,15,43,63 The expansion occurs due to the mutual repulsion of like-charged dust particles. Until now, experimental 10,13-15,63 and theoretical 43,47,64,65 studies of this expansion were for a dust cloud that initially filled a three-dimensional volume. A similar Coulomb expansion, of an initially three-dimensional plasma, occurs in ultracold

In this paper, a two-dimensional dust cloud is the initial condition in an experimental study. Unlike our previous afterglow

experiments that similarly began with a two-dimensional dust cloud, 53,54 here, we altered the experimental design, so that we could better observe the Coulomb expansion. In our previous experiment,<sup>54</sup> we were limited to observing the horizontal Coulomb expansion only to a barely measurable 0.4 mm, before the dust cloud impacted on the lower electrode at 700 mm/s. In the present experiment, we achieved an order-of-magnitude increase in the horizontal Coulomb expansion; we did this by slowing the fall of the cloud, using an upward electric force that opposed gravity, so that we could observe it for a longer time. This improvement allowed us to measure the Coulomb expansion adequately for testing a model. The model, based on Sheridan's equation of motion for a uniformly charged thin disk,<sup>70</sup> was found to accurately predict the expansion of the dust cloud at early times. As a further result, bouncing of dust particles on the electrode's surface was found to be suppressed by slowing the dust particles to <100 mm/s at impact.

We describe the experiment in Sec. II. Three kinds of results are presented in Sec. III: Coulomb expansion, thickening of the cloud, and suppression of the bounce. We describe a model of the Coulomb expansion in Sec. IV and compare it to experiment in Sec. V. A summary is provided in Sec. VI.

#### II. EXPERIMENT

#### A. Apparatus and procedure

Differently from the setup and procedure used in our previous experiments,  $^{53,54}$  here, we included an additional circuit for active control of the dc voltage on the lower electrode during the afterglow. We will discuss that additional circuit below. Otherwise, the setup and procedure were mostly the same as in our previous experiments, as we summarize here. Steady operation of the plasma was sustained by a peak-to-peak voltage of 312 V at 13 MHz. Most surfaces of the chamber were grounded, except for the lower electrode, where a dc self-bias of  $-150 \, \text{V}$  is developed. Due to this large self-bias, the sheath above this electrode included a substantial dc potential that provided a confining potential with dust particles levitated in a stable horizontal layer, during the steady operation of the plasma. The gas inside the plasma chamber was argon, at a low pressure of 8 mTorr.

The dust particles were melamine formaldehyde (MF) microspheres. Like other dusty plasma experimenters, we chose these polymer microspheres because they have a size dispersion that is a small percentage of the average diameter, and because they have only a very weak tendency to stick together in clumps of two or three, in a dry powder. For this experiment, the manufacturer's specifications<sup>77</sup> are a diameter of  $8.69 \,\mu\text{m}$ , with a size dispersion of  $0.11 \,\mu\text{m}$ . These dust particles were introduced into the plasma from above, by agitating a dispenser.

A negative charge developed on the dust particles when they were exposed to plasma under steady condition. As in other dusty plasma experiments,  $^{12,24,71-76}$  this charge allowed the dust particles to be levitated in the vertical direction and to be confined in the horizontal direction as well. The vertical levitation was due to a balance of the downward force of gravity and an upward electric force, which was sustained by a negative dc self-bias voltage on the lower electrode. Horizontal confinement was provided by a radial component in the natural electric field. The charge was measured in our previous experiment  $^{53}$  as  $-14\,000\,e$ , under the same plasma conditions, where e is the elementary charge.

Imaging of the dust particles was performed using two cameras, each with a laser sheet for illumination. Both cameras were Phantom model v5.2, with a 12-bit imaging sensor. For the top-view camera, illumination was provided by a 532-nm laser beam that was shaped into a horizontal sheet. The side-view camera was the most important camera for this experiment; it was operated at 1000 frames/s, and its field of view was  $42.35 \times 26.47 \, \mathrm{mm^2}$ . Its 55-mm focal-length lens was fitted with a 10-nm bandpass filter that admitted the 671-nm wavelength of a sheet of laser light, which was oriented in a vertical x-z plane. This vertical laser sheet had a thickness in the y-direction that we measured as 1.1 mm at the  $1/e^2$  points. Due to this finite thickness, dust particles tended to remain illuminated as they fell, despite slight displacements in the y-direction.

To prepare the initial two-dimensional horizontal layer of dust particles, we started by introducing only a few hundred or a few thousand dust particles, depending on the experimental run. By limiting the number of particles, we prevented the formation of a second layer above the layer of interest. As an additional step, after introducing the particles, we also used a standard sifting procedure to eliminate the heaviest of them. These heavier particles are typically clumps of two or more that stuck together after particles were dispensed into the plasma. The use of MF particles reduced the number of these heavy particles, but, nevertheless, some were introduced into the plasma, as we could see using the side-view camera because they were brighter than other particles, and they were levitated slightly lower as well.

To eliminate these heavy particles, our basic sifting procedure involves lowering the entire particle cloud. This is done by switching the rf power on and off at 1 kHz, with a duty cycle of about 10%. As a result, the particle layer is lowered, to a height that can be adjusted by varying the duty cycle, until the heaviest particles touch the lower electrode. Then, the switching is ceased, and the plasma is once again operated constantly. A single application of this sifting procedure reduces the number of heavy particles, especially the heaviest of them. After this sifting, for the most part, only single horizontal layer remains levitated under steady conditions, although a few particles that are heavier can remain, as we will mention again later.

To yield afterglow conditions, at time  $t\!=\!0$ , we turned off the rf power. This step is done by modulating the 13-MHz oscillator, as shown in Fig. 1. To monitor the afterglow conditions, the voltage on the lower electrode was recorded using a 100× probe and an oscilloscope. This measurement confirmed that the coupling capacitor  $C_{\text{coupl}}$  sustained, in large part, the negative dc self-bias of the lower electrode, after the rf power was turned off.

The plasma conditions in the afterglow developed over time. Electrons escaped the chamber volume first, leaving ion-rich conditions that reversed the charge polarity of the dust particles, as we described in Ref. 53. At that point, there was no longer a confining potential associated with a plasma sheath. By  $t=2\,\mathrm{ms}$ , the ions had largely escaped the chamber as well, and the electric field thereafter was that of a vacuum. The dust particles were still present at  $t=2\,\mathrm{ms}$ , and, in fact, they had moved very little prior to that time. Their charge was frozen, 53 with a positive value, prior to  $t=2\,\mathrm{ms}$ . Thereafter, the dust particles would experience two forces in the vertical direction: downward gravity and an electric force that was also downward, due to the negative potential on the lower electrode. In the horizontal direction, the dust particles repelled one another without screening

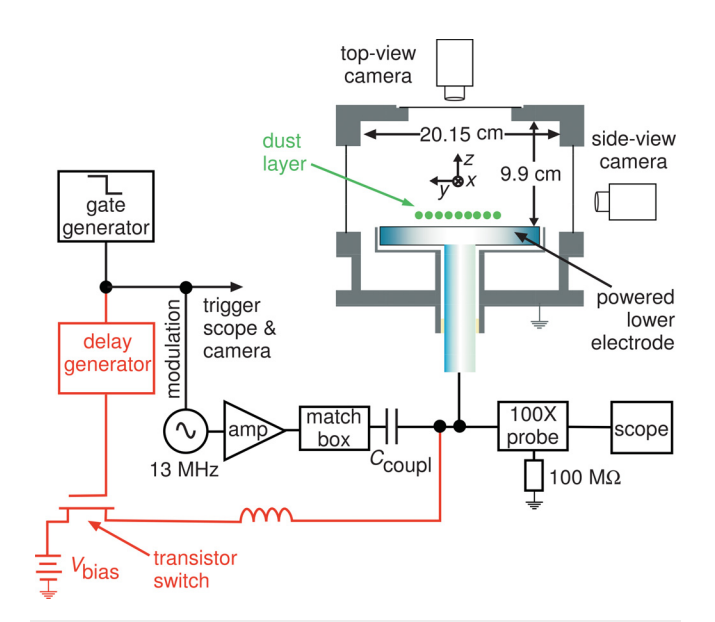


**FIG. 1.** Side-view sketch of the setup. During plasma operation, a layer of dust grains was levitated above the lower electrode that had a radio frequency voltage as well as a dc bias. A top-view camera imaged the entire cloud before it fell (illuminated by a horizontal sheet of 532-nm laser light, not shown here), allowing us to count the number N of particles and measure the cloud's diameter. A side-view camera imaged a vertical cross-section of the volume (illuminated by a vertical sheet of 671-nm laser light, not shown here), to capture the motion of dust particles within that cross section. During the afterglow, there was an upward electric field, which was due to our application of a positive dc bias  $V_{\rm bias}$  to the lower electrode, beginning at a time controlled by a delay generator and a transistor switch.

and without horizontal confinement, since the electrons and ions were no longer present.

The low gas pressure in our afterglow experiment is significant because it has been established theoretically that the expansion or explosion of a dust cloud is much reduced at high gas pressures. Early in the afterglow, the low gas density does not greatly impede the movement of ions and electrons to the chamber's boundaries, so that screening among dust particles ceased rapidly, and the interaction among dust particles, with their residual charges, would be in the "Coulomb interaction regime" not the "Yukawa interaction regime." Moreover, the dust particles did not experience much gas friction, as the cloud expanded.

Up to this point of our description, the experimental design was the same as in our previous experiments.  $^{53,54}$  For the present experiment, we improved the setup with an additional circuit to reverse the direction of the electric field, so that it was upward, in contrast to the downward direction during plasma operation. The direction of the electric field is established by the voltage on the lower electrode. Instead of allowing that voltage to have a negative value, as was established passively by the coupling capacitor  $C_{\rm coupl}$  in our previous experiments, the additional circuit actively controlled the lower electrode's potential, forcing it to a positive value, which was  $+160.1\,\rm V$ .

Components of this additional circuit are shown in Fig. 1. The additional circuit had its own dc power supply, which produced a potential  $V_{\rm bias}$  with respect to ground. This bias was applied at a time 2 ms after switching off the rf plasma. That time was chosen because

both electrons and ions had escaped the chamber, as judged by the voltage waveform on the lower electrode, so that only the dust particles remained at that point. This timing was set using a delay generator, which applied a 5 V bias to the gate of an N-channel power MOSFET, model IRFBG30. By applying this signal to its gate, the transistor went into conduction, having a drain-source voltage drop of 0.1 V. In order to block the rf voltage from reaching the transistor switch, during plasma operation, its output was connected to the lower electrode through an inductor, which was a toroidal ferrite core (Amidon FT-193-J) wound with 16 turns of wire. Upon application of the transistor switch, our oscilloscope measurements of the lower-electrode voltage revealed that the additional circuit overcame the charge on the coupling capacitor within 100  $\mu$ s, so that the lower-electrode potential thereafter remained fixed at +160.0 V, as compared to the ground potential of the other surfaces of the chamber. In this manner, the electric field was forced to have an upward direction, at a controlled level, by  $t = 2.1 \,\text{ms}$ .

# B. Electric field for controlled lifting

The electric field, for t > 2.1 ms, was calculated everywhere within the chamber using the numerical solution of Laplace's equation for this chamber. <sup>53</sup> An input for this calculation was the voltage on the lower electrode, which was measured using a 100X probe and an oscilloscope, shown in Fig. 1. The voltage waveform V(t) on the lower electrode, along with the time series for the calculated value of the electric field, is presented in Fig. 2.

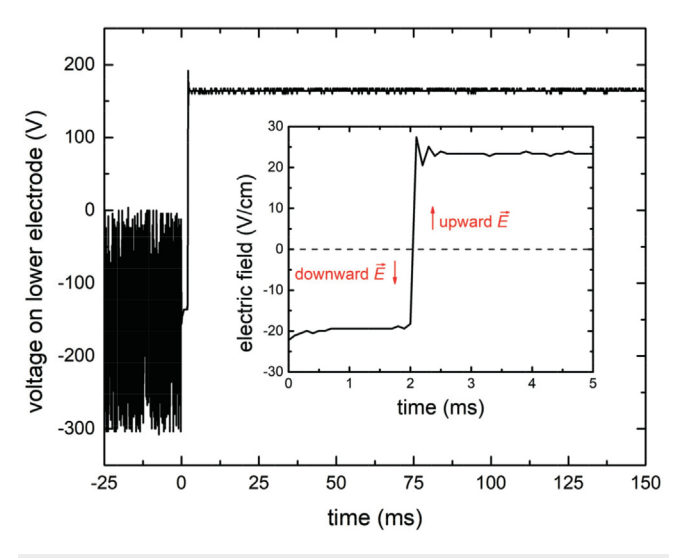


**FIG. 2.** Time series for the lower-electrode voltage (main graph) and the electric field at 8 mm above the lower electrode (inset). The rf power sustaining the plasma was turned off at t=0. Thereafter, during the first 2 ms, a negative dc voltage persisted on the lower electrode, due to capacitor  $C_{\rm coupl}$ . During that early time interval, electrons escaped the chamber first, so that some remaining ions collected on dust particles, charging them positively. Later, for t of order 2 ms, a dust particle's charge became frozen because both ions and electrons were absent; those late times the electric field was that of a vacuum. We chose to apply a positive potential  $V_{\rm bias} = +160 \, {\rm V}$  to the lower electrode, starting at  $t=2 \, {\rm ms}$ , for the purpose of applying a controlled upward electric lifting force, in opposition to gravity. The electrode voltage waveform shown in the main panel, recorded by the oscilloscope, was an input for our Laplace's equation calculation of the electric field, shown in the inset.

The lifting electric force, in opposition to gravity, occurs after the transistor switch causes the lower electrode to change in potential. As a step toward controlling this lifting force, one can adjust the electric field at a specific time, as we have done. For this experiment, we chose a potential of  $+160\,\mathrm{V}$ , which had an effect of reducing the downward acceleration. A greater positive voltage would be required to entirely inhibit the impact of the dust particles. The timing for this adjustment was chosen based on our estimation of the time required for the charge to "freeze" in the afterglow.

#### III. EXPERIMENTAL RESULTS

#### A. Dust cloud expansion

Four runs of experiments were carried out with different number of particles, N=404,578,1055, and 2100. All other starting conditions (including the rf power, dc voltage on the lower electrode, and height = 14.3 mm of the dust cloud) were the same for each run. By repeating the experiment with different numbers of particles, we will be able to test a model for the dust cloud's expansion, including its dependence on the number N of like-charged particles that repel one another.

Viewing from the side, we confirmed that the falling of the dust particles was slowed in this experiment by our reversal of the electric field. The particles took an average of 190 ms to impact on the lower electrode, in comparison to 40 ms in our previous experiment  $^{53}$  starting from the same height = 14.3 mm. This extended time, for the particles to fall, allowed us to observe the cloud of dust particles to expand noticeably, in the horizontal direction, as we discuss next.

The trajectories of dust particles can be seen in Fig. 3(a). This composite image is a superposition of video frames at an interval of 5 ms.

The particles fell with trajectories that curved prominently outward from the center, corresponding to an outward horizontal expansion.

Our measurement to quantify the horizontal expansion is summarized here. Using side-view camera images, we started by measuring a chord diameter L between the outermost dust particles. As an example, chord diameter is marked as the distance between arrows in Fig. 3(b). This chord diameter is less than the full diameter 2R of the dust cloud because the vertical laser sheet did not pass through the exact center of the particle cloud. To obtain R from our measurement of L, we used a simple geometrical calculation, described in the supplementary material. We repeated this measurement at  $5 \, \text{ms}$  intervals, yielding a time series R(t).

An example of the radial expansion R(t) is shown in Fig. 4, for the run with N = 578 particles. In that run, the cloud's diameter expanded by more than 50% by the time of impact. The nonlinear shape of the curve for R(t) indicates that the expansion accelerated, rather than having a steady outward velocity.

We can compare our observations for the expansion of a thin layer to previous theoretical and experimental results for a dust cloud that fills a fully three-dimensional volume. In the theoretical model of Piel and Goree, <sup>47</sup> the outer radius of a spherical cloud expands mostly at a steady speed, without the sustained acceleration seen in our experiment with a thin layer. In the afterglow experiment of Meyer and Merlino, <sup>14</sup> the expansion was seen mostly in the cloud's outermost particles, whereas in our thin layer, the entire cloud expanded proportionally (supplementary material). Also, the cloud in our experiment remained intact, instead of splitting or undergoing fission as in Ref. 15.

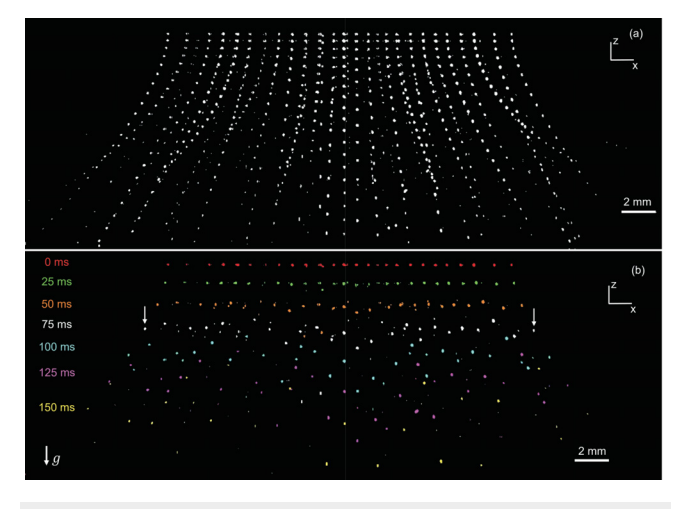


**FIG. 3.** Dust particles falling during the afterglow, in the presence of an upward electric field. Side-view images shown here are superimposed at intervals of (a) 5 and (b) 25 ms. Both panels are for the same experimental run, with N=578 dust particles, recorded at 1000 frames/s starting at t=0. The lower electrode surface is at the bottom edge of these images. An expansion of the dust cloud occurs in the horizontal direction, as is best seen in (a). To quantify the horizontal expansion, we measure a chord for the dust cloud as the distance L between the outermost dust particles, marked with arrows at t=75 ms. A thickening of the dust cloud also develops with time, as is best seen in (b). We tabulate the thickness as it develops over time in the supplementary material.

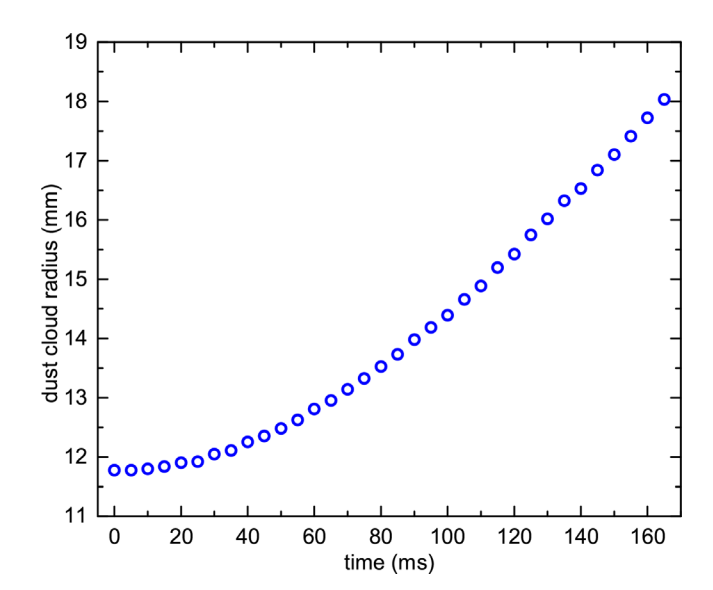


**FIG. 4.** Analysis results for radius R(t) of the dust cloud in an afterglow plasma. The cloud radius was obtained as one-half the width measured between outermost dust particles, as marked, for example, in Fig. 3(a). This measurement was adjusted to account for displacement of the illuminated cross section as compared to the dust cloud's center, as explained in supplementary material. These data, for the run with N=578 particles, reveal an acceleration in the dust cloud's expansion.

#### B. Thickening of dust cloud

In addition to expanding as it fell, the dust cloud also gradually became thicker. As can be seen in Fig. 3(b), some particles accelerated downward faster or slower than others.

To quantify the thickness, we calculate the rms thickness of a layer, as described in the supplementary material. This measure of the thickness gradually increased from 0.01 mm at the start of the fall, to 1.72 mm just before impact. In this analysis of the thickness, we excluded a few outlier particles, which were noticeably brighter and had unusually rapid vertical displacements, as can be seen in the video shown in the supplementary material. These outlier particles, which were <10% in number, were probably clumps of two or more particles that were not eliminated in the sifting procedure described in Sec. II A.

#### C. Suppressing the bounce

In this experiment, we also found conditions that suppress the bouncing of dust particles, when they impact the lower electrode. This bouncing, which was reported in our earlier paper,<sup>54</sup> was avoided in the present experiment, as can be seen in the video in the supplementary material. Suppressing the bounce was made possible by a lower impact velocity. In the present experiment, the impact velocity was less than 100 mm/s for most particles. (Only the bright outlier particles, which fell at a higher speed than most, were observed to bounce.) For comparison, in our previous experiment, particles impacted the lower electrode at 700 mm/s, and they all bounced.<sup>54</sup>

# IV. MODEL OF 2D DUST CLOUD EXPANSION

To model the expansion of the dust cloud, we adapt Sheridan's equation of motion for a planar dust disk.<sup>70</sup> That equation of motion is a combination of Eqs. (11) and (14) of Ref. 70. Sheridan's purpose was to describe the breathing mode, i.e., an oscillation of a dust cloud's diameter in the presence of a central confining potential, and in the presence of electrons and ions. Although we are not investigating the breathing mode here, Sheridan's equation of motion, nevertheless, provides a useful formulation for our purpose because it includes the effect of the collective Coulomb repulsion among dust particles, which tends to cause the dust cloud to expand, and because it assumes a suitable geometry for our experiment.

The geometry for Sheridan's equation of motion is a circular dust cloud that is thin, filling only a single layer. In contrast to his two-dimensional model, a description for the expansion of a three-dimensional spherical "Coulomb ball" was presented by Piel and Goree. The latter description is better suited for afterglow experiments that begin with fully three-dimensional dust clouds, as in Ref. 14.

Sheridan's equation of motion predicts how the dust cloud expands over time, taking into account several physical processes, including most importantly the Coulomb repulsion among all pairs of particles. Assumptions that underlie Sheridan's equation of motion are as follows:

- (1) The dust cloud's shape is a disk that is two dimensional, with negligible thickness.
- (2) The dust particles experience a frictional drag as they move through the gas background.

- (3) The dust disk expands uniformly, so that each inter-particle distance increases by the same proportion, as the disk diameter changes with time.
- (4) The Coulomb repulsion is resisted by an external harmonic confining electric potential. Electric forces from other sources are assumed to be negligible (for example, in our experiment, image charges on the distant electrode are insignificant due to their distance from the dust cloud greatly exceeding the interparticle distance within the dust cloud).
- (5) Rather than modeling the motion of individual particles, one can describe the dust cloud as a continuum using Eq. (11) of Ref. 70.
- (6) Electrons and ions are present, causing shielding with a characteristic Debye length λ, which diminishes the Coulomb repulsion among dust particles at great distances.

Assumption 1, a negligible thickness, is adequately satisfied in our experiment at early times, but it eventually fails, as we will discuss below. As a simplification, the frictional drag in assumption 2 can be ignored because at our low pressure of 8 mTorr, the frictional force amounts to less than 1% of the Coulomb force in our experiment, so that we can omit the corresponding term in Sheridan's equation of motion. For assumption 3, we confirmed that the interparticle distances expand uniformly (supplementary material). Regarding assumption 4, as a simplification, we will omit the harmonic confining force because that force arises from gradients in the background of electrons and ions, which were no longer present during the expansion of the dust cloud.

With these simplifications, Sheridan's equation of motion for the radius R(t) of a planar dust disk, with a total mass M and charge Q, is reduced to

$$\frac{M}{2}\frac{d^2R}{dt^2} - \frac{8}{3\pi}\frac{Q^2}{4\pi\varepsilon_0} \left[ \frac{1}{R^2} S\left(\frac{R}{\lambda}\right) - \frac{1}{R} S'\left(\frac{R}{\lambda}\right) \right] = 0. \tag{1}$$

The second term of Eq. (1) describes the interparticle Coulomb repulsion, retaining assumptions 1 and 3 listed above. In this second term, the dimensionless factor S is determined by a combination of the spatial arrangement of the dust particles and any Debye shielding that might diminish their Coulomb repulsion. An expression for the factor S is provided in Eq. (11) of Ref. 70, which makes use of the continuum approximation, i.e., assumption 5. We can further simplify Eq. (1) because assumption 6 for Debye shielding is no longer applicable after electrons and ions have escaped the chamber. Dust particles will interact among themselves with a simple Coulomb repulsion, so that we can set the Debye length to infinity in Eq. (11) of Ref. 70. With this simplification, S' becomes zero, and S(0) = 1.0058, which we obtained by numerically evaluating the integral in Eq. (11) of Ref. 70. Thus, during the dust cloud's expansion, Eq. (1) simplifies to

$$\frac{d^2 R}{dt^2} - \frac{2}{M} \frac{8}{3\pi} \frac{Q^2}{4\pi \varepsilon_0} \left[ \frac{1.0058}{R^2} \right] = 0.$$
 (2)

To use Eq. (2) as the equation of motion, three inputs are required to model our experiment: R(0), M, and Q. The initial radius R(0) was measured directly, using the top-view camera. The total mass M of the cloud was calculated simply as M = Nm, where N is the number of particles measured from the top-view camera at t = 0, and m is a single dust particle's mass as specified by the manufacturer. Finally, the

total charge Q = 10700 e of the cloud was obtained from a measurement of the downward acceleration, using Eq. (11) of Ref. 53.

We note that the frozen charge Q may actually have a distribution, varying from one particle to another. The value Q = 10700 e that we reported above was obtained, using the method of Ref. 53, as an average value, for multiple dust particles that were observed as they fell. As explained in Ref. 53, this value is largely determined by the mobility-limited ion velocity in the afterglow, after the electrons have departed. Not every ion moves exactly at that velocity, however, as the ion velocity actually has a finite distribution that is centered on that mobility-limited value. Accordingly, we expect that some dust particles may obtain a frozen charge that is slightly greater or less, depending on the energy of the last few ions that approach it, in the late stages of the afterglow. In other words, there will be a distribution of frozen charges, centered on the average value, due to the finite distribution of ion velocities in the late afterglow. We have not attempted to measure or model this distribution, but we can point out that as a percentage of the average charge, this effect should be smaller for a large average charge of 10 700 e as in the present experiment, than it would be for a much smaller average charge.

# V. COMPARISON OF MODEL AND EXPERIMENT

In Fig. 5, we compare the experimental measurements and model, for the dust cloud's expansion. The data for the model are from our numerical solution of Eq. (2), using a fourth-order Runge–Kutta integration, with no free parameters.

At early times, the experiment and model show good agreement in the value of R(t). For the dust cloud with  $N\!=\!400$ , this agreement persists for  $t\leq 70$  ms, with experiment and model differing by  $<\!1\%$  up to that point in time. For a larger dust cloud of  $N\!=\!2100$ , this agreement within 1% persists up to  $t\leq 35$  ms.

For longer times, the experiment and model gradually differ more and more. We are not able to explain this disagreement quantitatively, but we have considered one tendency, which is a thickening of the dust cloud layer, leading to a gradual failure of the twodimensionality approximation (i.e., assumption 1 as listed in Sec. IV). We note a coincidence of two different time intervals: the time required for the disagreement to develop to the 1% level in Fig. 5 and the time required for twice the rms thickness of the dust cloud to exceed the interparticle spacing. These two time intervals have about the same value, as shown in the supplementary material. One would intuitively expect that after thickening, two particles that are not in the same horizontal plane will experience a reduced radial component of their interparticle force because some of that interparticle force will be directed vertically. That reduction in the radial component would be expected to diminish the radial expansion in the experiment. However, we see the opposite tendency in Fig. 5, with the expansion in the experiment exceeding what was predicted by the model, at large t. Thus, the thickening of the layer cannot by itself explain the difference of experiment and model.

# VI. CONCLUSIONS

An afterglow experiment was designed to observe a thin dust cloud as it undergoes Coulomb expansion. We also observed a suppression of the bouncing of dust particles when they land.

Measuring the expansion required a longer observation time than in our previous experiments that started with a two-dimensional

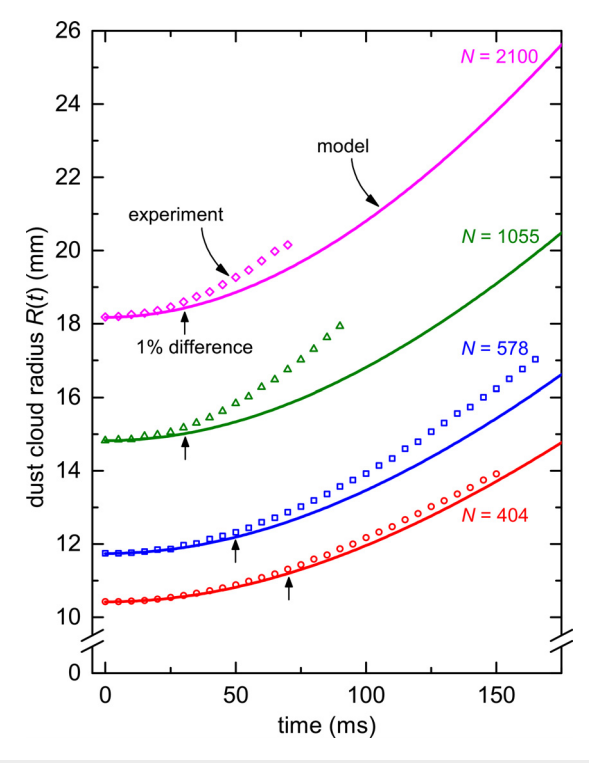


**FIG. 5.** Radius R(t) of the dust cloud as it expanded. Experimental data points, like those of Fig. 4, are compared to curves obtained from the two-dimensional model, Eq. (2). The four runs are distinguished by a different number N of dust particles and correspondingly a different initial radius R(0). Experimental data are shown up to time that we could no longer track the outermost particle due to its departure from the camera's field of view in the  $\pm x$  directions or due to its displacement in the  $\pm y$  directions outside the illumination layer. The theoretical curve is a numerical solution of Eq. (2) with no free parameters; its inputs are N and R(0) obtained from experimental top-view images, and charge  $Q = 10\,700\,e$  calculated from the experimentally measured acceleration. We find that the model, which assumes a thin 2D disk, agrees with the experiment within 1%, up to the time marked with arrows.

dust cloud. In those earlier experiments,  $^{53,54}$  the power sustaining the plasma was turned off abruptly at t=0, and the dust then fell downward with a high acceleration >1 g, impacting on the lower electrode after only about 40 ms. That time to impact was too short for the cloud to undergo a considerable horizontal expansion. In the present experiment, we increased the time to impact, to an average of 190 ms, by reversing the electric force beginning at t=2 ms, when the electrons and ions were gone. Falling much more slowly in this way, the dust cloud could be observed for a sufficient time to observe a considerable horizontal expansion.

Our measurement of the expansion allowed us to test a model. This model is our simplification of Sheridan's equation of motion  $^{70}$  for a 2D planar disk that is filled uniformly with charged dust. For early times, we found the radius predicted by the model agrees with the experiment within 1%. This agreement persisted up to a point in time, which was  $t\,{=}\,30$  to 70 ms depending on the particle number N. In this model, we retained the crucial term in Sheridan's equation of motion that describes the outward radial force due to Coulomb repulsion, but we omitted terms that are not applicable to our afterglow conditions.

As an additional result, we found that it is possible to suppress the bouncing of dust particles. At the low impact velocity of <100 mm/s in this experiment, the particles landed softly, without a bounce. In contrast to this result, in our previous experiment without a reversal of the electric force, 54 almost all particles bounced, after an impact velocity of typically 700 mm/s.

Our observation that bouncing of MF particles can be suppressed by reducing the impact velocity suggests that it may be feasible, in the future, to devise a scheme to transfer a crystallized structure of dust particles from the plasma to a solid surface, keeping the structure intact. Such an outcome would be of interest because we showed recently<sup>54</sup> that the crystalline structure of a single-layer dust cloud can survive at least 40 ms after extinguishing the electric power for the plasma. Transferring the crystalline structure permanently to the surface would require not only preventing a bounce, as we have demonstrated in this paper, but also reducing two other phenomena, Coulomb expansion and thickening of the dust cloud, which were observed in the present experiment and could disorganize the structure.

One advance in this paper is a step toward controlling an upward lifting force acting on dust particles in the afterglow. That force is the product of two quantities: the residual charge and electric field. The residual charge can be controlled by adjusting the potential on an electrode, as was demonstrated in Ref. 53. Here, we have shown that the electric field, after electrons and ions have departed, can be controlled by a delayed adjustment in an electrode potential. The timing for this delayed adjustment is governed by the physical process of "freezing" of the charge in the afterglow. We can suggest that a full control of the lifting force can be attained by separate adjustments of electrode potentials, the first to control the residual charge, and the second to control the electric field that then acts on that residual charge.

# SUPPLEMENTARY MATERIAL

See the supplementary material for a video of expansion of dust particles during fall, dust cloud radius calculation, dust cloud uniformity test, and dust cloud thickness measurement.

# **ACKNOWLEDGMENTS**

We thank F. Skiff for the use of a beam profiling camera and V. Zhuravlyov for helpful discussions. This work was supported by the Army Research Office under MURI Grant No. W911NF-18-1-0240, the United States Department of Energy under Grant No. DE-SC0014566 and NASA/JPL RSA No. 1672641, and the National Science Foundation under Grant No. PHY-1740379.

# **AUTHOR DECLARATIONS Conflict of Interest**

The authors have no conflicts to disclose.

#### **Author Contributions**

Neeraj Chaubey: Conceptualization (equal); Data curation (lead); Formal analysis (lead); Investigation (equal); Methodology (equal); Writing - original draft (equal); Writing - review & editing (equal). John Goree: Conceptualization (equal); Investigation (equal); Methodology (equal); Supervision (lead); Writing - original draft (equal); Writing - review & editing (equal).

#### **DATA AVAILABILITY**

The data that support the findings of this study are available within the article and its supplementary material.

# **REFERENCES**

- <sup>1</sup>P. K. Shukla and A. A. Mamun, Introduction to Dusty Plasma Physics, Series in Plasma Physics (Institute of Physics Publishing, 2001).
- <sup>2</sup>P. M. Bellan, Fundamentals of Plasma Physics (Cambridge University Press, 2008), Chap. 17, pp. 483-506.
- <sup>3</sup>A. Piel, "Chapter 10: Dusty plasmas," in Plasma Physics: An Introduction to Laboratory, Space, and Fusion Plasmas (Springer, Berlin, 2010), pp. 259-321.
- <sup>4</sup>A. Melzer, *Physics of Dusty Plasmas*, Lecture Notes in Physics (Springer International Publishing, Cham, 2019), Vol. 962.
- <sup>5</sup>V. E. Fortov, A. G. Khrapak, S. A. Khrapak, V. I. Molotkov, and O. F. Petrov, "Dusty plasmas," Phys.-Usp. 47, 447-492 (2004).
- <sup>6</sup>V. N. Tsytovich, G. E. Morfill, S. V. Vladimirov, and H. M. Thomas, "Elementary processes in complex plasmas," in Elementary Physics of Complex Plasmas (Springer, Berlin, Heidelberg, 2008), pp. 67-140.
- <sup>7</sup>A. Melzer and J. Goree, "Chapter 6: Fundamentals of dusty plasmas," in *Low* Temperature Plasmas: Fundamentals, Technologies and Techniques, 2nd ed., edited by R. Hippler, H. Kersten, M. Schmidt, and K. H. Schoenbach (Wiley-VCH, Weinheim, 2008), p. 129.
- <sup>8</sup>M. Bonitz, C. Henning, and D. Block, "Complex plasmas: A laboratory for strong correlations," Rep. Prog. Phys. 73, 066501 (2010).
- <sup>9</sup>M. Choudhary, "Perspective: Dusty plasma experiments—A learning tool for
- physics graduate students," Eur. J. Phys. 42, 053001 (2021).

  A. Barkan and R. L. Merlino, "Confinement of dust particles in a double layer," Phys. Plasmas 2, 3261-3265 (1995).
- <sup>11</sup>T. Antonova, S. A. Khrapak, M. Y. Pustylnik, M. Rubin-Zuzic, H. M. Thomas, A. M. Lipaev, A. D. Usachev, V. I. Molotkov, and M. H. Thoma, "Particle charge in PK-4 dc discharge from ground-based and microgravity experiments," Phys. Plasmas 26, 113703 (2019).
- <sup>12</sup>E. Thomas, U. Konopka, R. L. Merlino, and M. Rosenberg, "Initial measurements of two- and three-dimensional ordering, waves, and plasma filamentation in the magnetized dusty plasma experiment," Phys. Plasmas 23, 055701 (2016).
- <sup>13</sup>R. L. Merlino, J. K. Meyer, K. Avinash, and A. Sen, "Coulomb fission of a dusty plasma," Phys. Plasmas 23, 064506 (2016).

  14 J. K. Meyer and R. L. Merlino, "Evolution of dust clouds in afterglow plasmas,"
- IEEE Trans. Plasma Sci. 44, 473-478 (2016).
- <sup>15</sup>R. L. Merlino, J. K. Meyer, A. Barkan, K. Avinash, and A. Sen, "Coulomb explosion and fission of charged dust clusters," AIP Conf. Proc. 1925, 020021 (2018).
- <sup>16</sup>M. Choudhary, R. Bergert, S. Mitic, and M. H. Thoma, "Three-dimensional dusty plasma in a strong magnetic field: Observation of rotating dust tori," Phys. Plasmas 27, 063701 (2020).
- <sup>17</sup>M. Kaur, S. Bose, P. Chattopadhyay, D. Sharma, J. Ghosh, and Y. Saxena, "Observation of dust torus with poloidal rotation in direct current glow discharge plasma," Phys. Plasmas 22, 033703 (2015).
- <sup>18</sup>M. Kaur, S. Bose, P. Chattopadhyay, D. Sharma, J. Ghosh, Y. Saxena, and E. Thomas, Jr., "Generation of multiple toroidal dust vortices by a non-monotonic density gradient in a direct current glow discharge plasma," Phys. Plasmas 22, 093702 (2015).
- <sup>19</sup>S. Arumugam, P. Bandyopadhyay, S. Singh, M. Hariprasad, D. Rathod, G. Arora, and A. Sen, "DPEx-II: A new dusty plasma device capable of producing large sized DC Coulomb crystals," Plasma Sources Sci. Technol. 30, 085003
- <sup>20</sup>B. Chutia, T. Deka, Y. Bailung, D. Sharma, S. K. Sharma, and H. Bailung, "Spatiotemporal evolution of a self-excited dust density wave in a nanodusty plasma under strong Havnes effect," Phys. Plasmas 28, 123702 (2021).
- <sup>21</sup>D. Samsonov, J. Goree, H. M. Thomas, and G. E. Morfill, "Mach cone shocks in a two-dimensional Yukawa solid using a complex plasma," Phys. Rev. E 61, 5557-5572 (2000).

- <sup>22</sup>S. Nunomura, D. Samsonov, and J. Goree, "Transverse waves in a two-dimensional screened-Coulomb crystal (dusty plasma)," Phys. Rev. Lett. 84, 5141–5144 (2000).
- <sup>23</sup>G. A. Hebner, M. E. Riley, and K. E. Greenberg, "Analysis of the particle interactions in a two-dimensional-plasma dust crystal and the use of dust as a probe of the time-averaged presheath electric field," Phys. Rev. E 66, 046407 (2002).
- <sup>24</sup>V. Nosenko, J. Goree, Z. W. Ma, D. H. E. Dubin, and A. Piel, "Compressional and shear wakes in a two-dimensional dusty plasma crystal," Phys. Rev. E 68, 056409 (2003).
- <sup>25</sup>P. Hartmann, G. J. Kalman, Z. Donkó, and K. Kutasi, "Equilibrium properties and phase diagram of two-dimensional Yukawa systems," Phys. Rev. E 72, 026409 (2005).
- <sup>26</sup>C. A. Knapek, D. Samsonov, S. Zhdanov, U. Konopka, and G. E. Morfill, "Recrystallization of a 2D plasma crystal," Phys. Rev. Lett. 98, 015004 (2007).
- <sup>27</sup>W. D. S. Ruhunusiri, J. Goree, Y. Feng, and B. Liu, "Polygon construction to investigate melting in two-dimensional strongly coupled dusty plasma," Phys. Rev. E 83, 066402 (2011).
- <sup>28</sup>V. Singh Dharodi, S. K. Tiwari, and A. Das, "Visco-elastic fluid simulations of coherent structures in strongly coupled dusty plasma medium," Phys. Plasmas 21, 073705 (2014).
- <sup>29</sup>E. Kostadinova, F. Guyton, A. Cameron, K. Busse, C. Liaw, L. Matthews, and T. Hyde, "Transport properties of disordered two-dimensional complex plasma crystal," Contrib. Plasma Phys. 58, 209–216 (2018).
- <sup>30</sup> A. Kananovich and J. Goree, "Shocks propagate in a 2D dusty plasma with less attenuation than due to gas friction alone," Phys. Plasmas 27, 113704 (2020).
- <sup>31</sup>A. Kananovich and J. Goree, "Experimental determination of shock speed versus exciter speed in a two-dimensional dusty plasma," Phys. Rev. E 101, 043211 (2020).
- <sup>32</sup>M. G. Hariprasad, P. Bandyopadhyay, G. Arora, and A. Sen, "Experimental investigation of test particle induced micro-structural changes in a finite twodimensional complex plasma crystal," Phys. Plasmas 26, 103701 (2019).
- 33M. G. Hariprasad, P. Bandyopadhyay, G. Arora, and A. Sen, "Experimental observation of a first-order phase transition in a complex plasma monolayer crystal," Phys. Rev. E 101, 043209 (2020).
- <sup>34</sup>V. S. Dharodi, "Rotating vortices in two-dimensional inhomogeneous strongly coupled dusty plasmas: Shear and spiral density waves," Phys. Rev. E 102, 043216 (2020).
- 35M. Choudhary, R. Bergert, S. Moritz, S. Mitic, and M. H. Thoma, "Rotational properties of annulus dusty plasma in a strong magnetic field," Contrib. Plasma Phys. 61, e202000110 (2021).
- <sup>36</sup>S. Singh, P. Bandyopadhyay, K. Kumar, and A. Sen, "Square lattice formation in a monodisperse complex plasma," Phys. Rev. Lett. **129**, 115003 (2022).
- <sup>37</sup>M. A. Childs and A. Gallagher, "Plasma charge-density ratios in a dusty
- plasma," J. Appl. Phys. 87, 1086–1090 (2000).
  38 A. V. Ivlev, M. Kretschmer, M. Zuzic, G. E. Morfill, H. Rothermel, H. M. Thomas, V. E. Fortov, V. I. Molotkov, A. P. Nefedov, A. M. Lipaev, O. F. Petrov, Y. M. Baturin, A. I. Ivanov, and J. Goree, "Decharging of complex plasmas: First kinetic observations," Phys. Rev. Lett. 90, 055003 (2003).
- <sup>39</sup>L. Couëdel, M. Mikikian, L. Boufendi, and A. A. Samarian, "Residual dust charges in discharge afterglow," Phys. Rev. E 74, 026403 (2006).
- <sup>40</sup>L. Couedel, A. A. Samarian, M. Mikikian, and L. Boufendi, "Influence of the ambipolar-to-free diffusion transition on dust particle charge in a complex plasma afterglow," Phys. Plasmas 15, 063705 (2008).
- <sup>41</sup>L. Couëdel, A. Mezeghrane, A. Samarian, M. Mikikian, Y. Tessier, M. Cavarroc, and L. Boufendi, "Complex plasma afterglow," Contrib. Plasma Phys. 49, 235–259 (2009).
- <sup>42</sup>I. V. Schweigert and A. L. Alexandrov, "Effect of nanoparticles on an rf discharge afterglow," J. Phys. D 45, 325201 (2012).
- 43V. Saxena, K. Avinash, and A. Sen, "Dust cluster explosion," Phys. Plasmas 19, 093706 (2012).
- <sup>44</sup>I. B. Denysenko, I. Stefanović, B. Sikimić, J. Winter, and N. A. Azarenkov, "Discharging of dust particles in the afterglow of plasma with large dust density," Phys. Rev. E 88, 023104 (2013).
- <sup>45</sup>I. B. Denysenko, H. Kersten, and N. A. Azarenkov, "Electron energy distribution function, effective electron temperature, and dust charge in the temporal afterglow of a plasma," Phys. Plasmas 23, 053704 (2016).

- <sup>46</sup>I. B. Denysenko, N. A. Azarenkov, K. Ostrikov, and M. Y. Yu, "Electron energy probability function in the temporal afterglow of a dusty plasma," Phys. Plasmas 25, 013703 (2018).
- <sup>47</sup>A. Piel and J. A. Goree, "Collisional and collisionless expansion of Yukawa balls," Phys. Rev. E 88, 063103 (2013).
- <sup>48</sup>M. Chaudhuri, L. Couëdel, J. A. Edward Thomas, P. Huber, A. M. Lipaev, H. M. Thomas, and M. Schwabe, "Spontaneous dust pulse formation in the afterglow of complex plasmas under microgravity conditions," arXiv:2103.09607 (2021).
- <sup>49</sup>I. B. Denysenko, M. Mikikian, and N. A. Azarenkov, "Dust dynamics during the plasma afterglow," J. Phys. D 55, 095201 (2021).
- 50 E. Husmann, E. Thimsen, and X. Chen, "Particle charge distributions in the effluent of a flow-through atmospheric pressure low temperature plasma," Plasma Sources Sci. Technol. 30, 075030 (2021).
- <sup>51</sup>J. C. A. van Huijstee, P. Blom, A. T. A. Peijnenburg, and J. Beckers, "Spatio-temporal plasma afterglow induces additional neutral drag force on micro-particles," Front. Phys. 10, 926160 (2022).
- <sup>52</sup>L. Wörner, A. V. Ivlev, L. Couëdel, P. Huber, M. Schwabe, T. Hagl, M. Mikikian, L. Boufendi, A. Skvortsov, A. M. Lipaev, V. I. Molotkov, O. F. Petrov, V. E. Fortov, H. M. Thomas, and G. E. Morfill, "The effect of a direct current field on the microparticle charge in the plasma afterglow," Phys. Plasmas 20, 123702 (2013).
- <sup>53</sup>N. Chaubey, J. Goree, S. J. Lanham, and M. J. Kushner, "Positive charging of grains in an afterglow plasma is enhanced by ions drifting in an electric field," Phys. Plasmas 28, 103702 (2021).
- <sup>54</sup>N. Chaubey and J. Goree, "Preservation of a dust crystal as it falls in an afterglow plasma," Front. Phys. 10, 879092 (2022).
  <sup>55</sup>T. J. A. Staps, "A review of nanoparticle decharging in atmospheric pressure
- 55T. J. A. Staps, "A review of nanoparticle decharging in atmospheric pressure plasma afterglows," Front. Phys. 10, 988812 (2022).
- 56 L. Couëdel, "Temporal dusty plasma afterglow: A review," Front. Phys. 10, 913 (2022).
- <sup>57</sup>B. van Minderhout, J. C. A. van Huijstee, B. Platier, T. Peijnenburg, P. Blom, G. M. W. Kroesen, and J. Beckers, "Charge control of micro-particles in a shielded plasma afterglow," Plasma Sources Sci. Technol. 29, 065005 (2020).
- <sup>58</sup>B. van Minderhout, J. C. A. van Huijstee, A. T. A. Peijnenburg, P. Blom, G. M. W. Kroesen, and J. Beckers, "Charge neutralisation of microparticles by pulsing a low-pressure shielded spatial plasma afterglow," Plasma Sources Sci. Technol. 30, 045016 (2021).
- <sup>59</sup>B. van Minderhout, T. Peijnenburg, P. Blom, J. M. Vogels, G. M. W. Kroesen, and J. Beckers, "The charge of micro-particles in a low pressure spatial plasma afterglow," J. Phys. D **52**, 32LT03 (2019).
- <sup>60</sup>V. Schneider, "Optisch gefangene Mikropartikel als Sonden in einem Hochfrequenz-Niederdruckplasma," Ph.D. thesis (University of Kiel, 2020).
- <sup>61</sup>G. Sharma, N. Abuyazid, S. Dhawan, S. Kshirsagar, R. M. Sankaran, and P. Biswas, "Characterization of particle charging in low-temperature, atmospheric-pressure, flow-through plasmas," J. Phys. D 53, 245204 (2020).
- <sup>62</sup>V. Suresh, L. Li, J. R. G. Felipe, and R. Gopalakrishnan, "Modeling nanoparticle charge distribution in the afterglow of non-thermal plasmas and comparison with measurements," J. Phys. D 54, 275205 (2021).
- <sup>63</sup>T. Antonova, C.-R. Du, A. V. Ivlev, B. M. Annaratone, L.-J. Hou, R. Kompaneets, H. M. Thomas, and G. E. Morfill, "Microparticles deep in the plasma sheath: Coulomb 'explosion'," Phys. Plasmas 19, 093709 (2012).
- 64 A. V. Ivlev, "Coulomb expansion: Analytical solutions," Phys. Rev. E 87, 025102 (2013).
- <sup>65</sup>A. Piel, "Plasma crystals: Experiments and simulation," Plasma Phys. Controlled Fusion 59, 014001 (2016).
- 66 T. C. Killian, "Ultracold neutral plasmas," Science 316, 705–708 (2007).
- <sup>67</sup>D. Murphy, R. W. Speirs, D. V. Sheludko, C. T. Putkunz, A. J. McCulloch, B. M. Sparkes, and R. E. Scholten, "Detailed observation of space-charge dynamics using ultracold ion bunches," Nat. Commun. 5, 4489 (2014).
- <sup>68</sup>M. A. Viray, S. A. Miller, and G. Raithel, "Coulomb expansion of a cold non-neutral rubidium plasma," Phys. Rev. A 102, 033303 (2020).
- <sup>69</sup>V. S. Dharodi and M. S. Murillo, "Sculpted ultracold neutral plasmas," Phys. Rev. E 101, 023207 (2020).
- <sup>70</sup>T. E. Sheridan, "Theory for the breathing mode of a complex plasma disk," Phys. Plasmas 11, 5520–5524 (2004).

- <sup>71</sup>H. Thomas, G. E. Morfill, V. Demmel, J. Goree, B. Feuerbacher, and D. Möhlmann, "Plasma crystal: Coulomb crystallization in a dusty plasma," Phys. Rev. Lett. 73, 652–655 (1994).
- 72T. Trottenberg, A. Melzer, and A. Piel, "Measurement of the electric charge on particulates forming Coulomb crystals in the sheath of a radiofrequency plasma," Plasma Sources Sci. Technol. 4, 450–458 (1995).

  73
  E. Thomas and M. Watson, "Charging of silica particles in an argon dusty
- plasma," Phys. Plasmas 7, 3194–3197 (2000).

  74S. Ratynskaia, S. Khrapak, A. Zobnin, M. H. Thoma, M. Kretschmer, A. Usachev, V. Yaroshenko, R. A. Quinn, G. E. Morfill, O. Petrov, and
- V. Fortov, "Experimental determination of dust-particle charge in a discharge plasma at elevated pressures," Phys. Rev. Lett. 93, 085001
- 75X. Wang, J. Colwell, M. Horanyi, and S. Robertson, "Charge of dust on surfaces in plasma," IEEE Trans. Plasma Sci. 35, 271-279 (2007).
- 76 A. Douglass, V. Land, L. Matthews, and T. Hyde, "Dust particle charge in plasma with ion flow and electron depletion near plasma boundaries," Phys. Plasmas 18, 083706 (2011).
- 77 See http://www.microparticles.de/ for "Purchased from Microparticles GmbH, Volmerstr. 9A, D-12489 Berlin, Germany."